Journal of ELECTRONIC MATERIALS, Vol. 36, No. 7, 2007
DOI: 10.1007/s11664-007-0154-0
© 2007 TMS

Thermoelectric Properties of Na_xCoO_2 and Prospects for Other Oxide Thermoelectrics

D.J. SINGH[1,3] and D. KASINATHAN[2]

1.—Materials Science and Technology Division, Oak Ridge National Laboratory, Oak Ridge, TN 37831-6032, USA. 2.—Department of Physics, University of California, Davis, CA 95616, USA. 3.—e-mail: Singhdj@ornl.gov

We discuss the thermoelectric properties of Na_xCoO_2 using the electronic structure, as determined in first principles calculations, and Boltzmann kinetic transport theory. The Fermi energy lies near the top of a manifold of Co t_{2g} bands. These t_{2g} bands are separated by a large gap from the higher-lying e_g states. Although the large crystal-field splitting implies substantial Co–O hybridization, the bands are narrow. Application of standard Boltzmann transport theory to such a narrow band structure yields high thermopowers in accord with experimental observations, even for high metallic carrier densities. The high thermopowers observed for Na_xCoO_2 can therefore be explained by standard band theory and do not rely on low dimensionality or correlation effects specific to Co. We also present results for the cubic spinel structure $ZnRh_2O_4$. Like Na_xCoO_2, this compound has very narrow valence bands. We find that if it could be doped with mobile carriers, it would also have a high thermopower, comparable with that of Na_xCoO_2.

Key words: Na_xCoO_2, $ZnRh_2O_4$, thermoelectric, band structure

The layered Co oxide, Na_xCoO_2, has remarkable transport properties[1] that have stimulated much experimental and theoretical work. In particular, it has a high thermopower and a high thermoelectric figure of merit, ZT, even though it has a metallic carrier density, $h \approx 10^{22}$ cm^{-3}, in contrast with h 10^{19}–10^{20} cm^{-3} for traditional thermoelectrics. Since the discovery of the high ZT of Na_xCoO_2 several misfit cobaltate compounds with hexagonal CoO_2 sheets that are structurally similar to those in Na_xCoO_2 have been found.[2–4] No other high ZT oxides have yet been reported, however. It is, therefore, important to understand what special features of these cobaltates are responsible for the high thermoelectric performance.

The hexagonal crystal structure of Na_xCoO_2 consists of hexagonal Co sheets, coordinated above and below (along the c-axis) with hexagonal O sheets to produce octahedral coordination of the Co. These CoO_2 blocks are stacked in alternating fashion, i.e. for the stacking ...–O–Co–O—O–Co–O–... one has ...*ABC–CBA*.... This yields two different types of trigonal prismatic sites between the sheets, one over the Co ions (B) and the other over the O in the layer on the opposite side of the Co sheet. These are both partially occupied by Na. Here we denote the Na sites above Co as Na_{Co} and those above the holes as Na_h. There is one Na_{Co} and one Na_h site per Co, with a total Na filling of x per Co, or $x/2$ per site. The number of available sites is smaller, however, because occupation of neighboring Co sites is highly unfavorable owing to the short Na–Na distance that would result.

The band structure[5] of Na_xCoO_2 ($x = 0.5$) as calculated within the local density approximation (LDA), using a virtual crystal approximation, shows well separated manifolds of O $2p$, Co t_{2g}, and Co e_g bands, with the Fermi energy near the top of the t_{2g} manifold. This is shown in Figs. 1 and 2. The valence and conduction bands may be seen to be highly anisotropic, with much less dispersion along the c-axis direction than in the ab-plane. This is consistent with transport and other measurements, which are indicative of much lower conductivity in the c-direction than in the plane.[1] Because of this, transport in polycrystalline material is dominated

(Received October 11, 2006; accepted March 16, 2007; published online June 13, 2007)

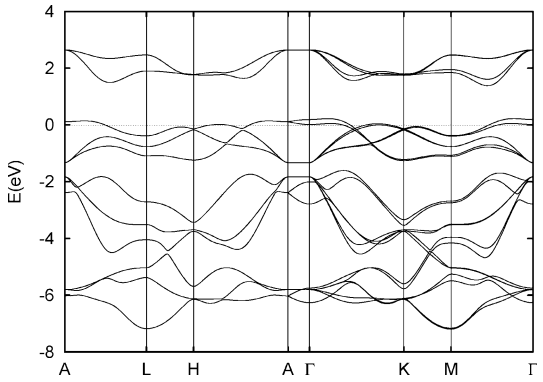

Fig. 1. Local density approximation band structure of $Na_{0.5}CoO_2$ as obtained within the virtual crystal approximation. The Fermi energy is denoted by the *dashed horizontal line* at 0 eV.

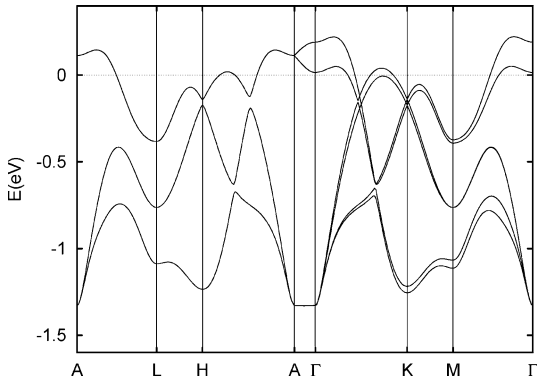

Fig. 2. Band structure of $Na_{0.5}CoO_2$, as in Fig. 1, with an expanded energy scale covering the t_{2g} manifold.

by the *ab*-plane coefficients, and single crystals have the best thermoelectric performance for current in the *ab*-plane.

The size of the gap, 1.3 eV, between the Co t_{2g} and e_g manifolds deserves mention. Crystal-field splittings in oxides are mainly because of transition metal–O hybridization. Because, with geometrical factors, the same type of hybridization contributes to band widths (which then narrow the gaps) andcrystal field splittings, it is unusual to have such large crystal-field gaps. The layered structure of Na_xCoO_2, which consists of edge-shared octahedra with near 90-degree Co–O–Co bonds, favors narrow bands[6] even though there is substantial hybridization. This special arrangement thus results in the large gap found in the calculations.

As is apparent from the valence band structure, Fig. 2, two bands cross the Fermi energy. One gives a large hole Fermi surface around the zone center and the other gives a set of small pockets along the Γ–K/A–H directions. In the hexagonal structure the site symmetry of Co is rhombohedral so there is a secondary lifting of degeneracy in the t_{2g} manifold into a single-degenerate a_g symmetry and a twofold-degenerate e_g symmetry, denoted e_g' here to distinguish it from the higher lying e_g manifold produced by the primary crystal field. The a_g-derived band yields the large hole sections of the Fermi surface around the zone center (note there are two CoO_2 sheets per unit cell and, therefore, two sets of bands—degenerate in the $k_z = 1/2$ plane and split into even and odd combinations in the $k_z = 0$ plane). The e_g' bands yield the small hole pockets along the Γ–K directions. This basic Fermi surface structure persists over a wide range of x. Whereas the small e_g' sections have low velocities and, therefore, are not expected to make significant direct contributions to transport, they would contribute to thermodynamic quantities, susceptibility, and other phase space-dependent properties, especially at low x, where they are two-dimensional and highly nested.[7] In any case, while the small sections are clearly present in LDA calculations, they have not been observed in photoemission. Instead, angle-resolved photoemission (ARPES) experiments see a large section of Fermi surface consistent with the a_g sheets and a dispersive band that approaches the Fermi level (E_F) but then shows a kink-like feature and continues below E_F.[8,9] This discrepancy between LDA predictions and ARPES measurements may be the result of Na disorder in Na_xCoO_2 samples,[10] based on supercell calculations of the potential variation because of Na disorder. This disorder would also be a source of scattering, which would reduce the carrier mobility. Point defect scattering in metals is not usually strongly energy dependent; we do not, therefore, expect this scattering to affect the constant scattering time approximation used here for calculation of the thermopower.

High values of the thermoelectric figure of merit, $ZT = \sigma S^2 T/\kappa$ (T is the temperature, S is the thermopower, σ is the electrical conductivity, and κ is the thermal conductivity) cannot be obtained without high values of S. This is because the thermal conductivity contains an electronic part, which is normally given by the Wiedemann–Franz relationship, $\kappa = L\sigma T$, where L is the Lorentz number. Thus an essential aspect of the thermoelectric performance of Na_xCoO_2 is the high values of the thermopower observed in this material, even at high carrier density. Within Boltzmann transport theory[11] the thermopower at low temperature is proportional to temperature and the logarithmic derivative of the conductivity with energy, ε,

$$S_{\alpha\beta} = (\pi^2 k^2 T/3e) \sum_{\gamma} (\sigma^{-1})_{\alpha\gamma} \frac{d\sigma_{\gamma\beta}}{d\varepsilon}$$

Here, $S_{\alpha\beta}$ is the Seebeck tensor, k is the Boltzmann constant and $\sigma_{\alpha\beta}$ is the conductivity tensor. At higher temperatures the expression is more complicated, involving integration over an

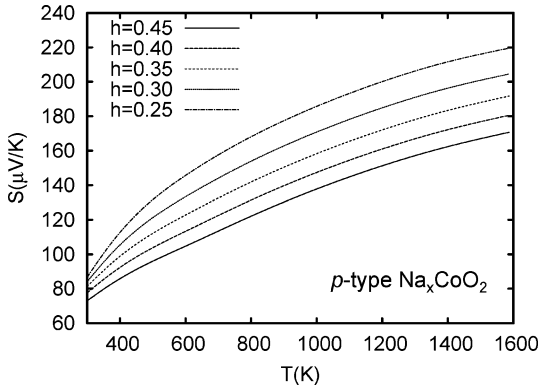

Fig. 3. Calculated $S(T)$ for hole-doped Na_xCoO_2 based on application of Boltzmann theory, within the constant scattering time approximation, and using a rigid band model based on the virtual crystal band structure of $Na_{0.67}CoO_2$. h is the hole-doping level on a per Co basis. It is nominally related to the Na concentration, x, by $h = 1-x$, but oxygen and other compensating defects may alter the relationship between x and h, depending on sample preparation.

energy range on the scale of a few kT;[11,12] it still, nonetheless, connects high thermopower to strong variation of the conductivity with energy on this scale. Thus the high thermopowers observed in Na_xCoO_2 could be because of the narrow bandwidth. In fact, it was found[5] that high values of $S(T)/T$ are obtained by applying the low-temperature Boltzmann expression within the constant scattering time approximation to the band structure calculated for $x = 0.5$. Here we present calculations including the full temperature dependence, performed at a variety of doping levels, on the basis of the band structure calculated for $x = 0.67$.

Figure 3 shows the $S(T)$ calculated for transport in the ab-plane (i.e. perpendicular to the hexagonal axis) for a variety of doping levels, including the range of x typical of thermoelectric samples. This was obtained by using a virtual crystal band structure for $x = 0.67$ (this is similar to that at $x = 0.5$ with a shift in the relative positions of the two Fermi surfaces and in the Fermi energy, as discussed elsewhere[6]). The band structure was calculated with the linearized augmented planewave (LAPW) method including local orbital extensions.[13–15] The computational details are similar to those in Ref. 6 Thus the reported results for the thermopower are based on a band structure calculation for $x = 0.67$, with a virtual crystal approximation with a virtual atom $Z = 10.67$. Transport coefficients were obtained by using the BoltzTrap code[12] and applying the constant scattering time approximation. A dense grid of approximately 11,000 k-points in the Brillouin zone was used to obtain convergence. With the constant scattering time approximation, the absolute $S(T)$ is obtained directly from the band structure with no adjustable terms. This is because the conductivity is proportional to the scattering time, which then cancels in the logarithmic derivative. It is apparent that high values of the thermopower are obtained, in reasonable accord with experimental values. This leads to the conclusion that the high thermopowers observed for Na_xCoO_2 can be explained by standard local density approximation band structures and the usual kinetic transport theory for metals. The high values at high carrier density are a direct result of the narrow t_{2g} bands in this material, which in turn results from the bonding topology. This mechanism does not rely directly on strong correlation effects associated with Co ions. It has been assumed that the transport in Na_xCoO_2 is strongly dependent on strong correlation effects, mostly because it was assumed that standard transport theory cannot explain the high thermopowers observed. The current results show that this is incorrect. Instead, strong correlations, which may well be present, are not essential for the high thermopower in Na_xCoO_2.

This raises the question of whether other non-Co-based oxides with high thermopowers and high ZT exist. There are many oxides that form in structures with only near 90-degree metal–O–metal bond angles and large metal–metal separations. One such structure is the normal spinel structure, AB_2O_4, assuming the transition element is on the B-site and that the A-site ion is inert in the sense of not participating substantially in the valence electronic structure. Also, the spinel structure is cubic, which is advantageous for thermoelectric applications, because the relevant transport coefficients are then isotropic and oriented single crystals and/or highly oriented ceramic would not be required. $ZnRh_2O_4$ is one such material. It occurs in the cubic spinel structure with Rh on the B-site. Unlike Na_xCoO_2 it is an insulator and, as far as we are aware, doping with mobile carriers to obtain metallic conductivity has not been reported, although p-type conduction has been observed.[16] Alloying the Zn A-site with monovalent ions, for example Li or Tl may introduce holes, but it is not known whether this can be done in a way that would lead to metallic properties. According to LDA band structure calculations and optical measurements,[17] $ZnRh_2O_4$ has a narrow t_{2g}-derived valence band manifold, with a width similar to that of Na_xCoO_2 and, also like Na_xCoO_2, it has a large crystal-field gap between the valence and conduction e_g bands, which reflects strong Rh–O hybridization. This is not unexpected, because Rh lies directly below Co in the periodic table. Because Rh is a 4d element, stronger hybridization with ligands relative to the 3d analog is expected, and correlation effects associated with on-site Coulomb repulsion should be weaker. As mentioned, the t_{2g} valence band structure, shown in Fig. 4, has a width similar to that of Na_xCoO_2. The detailed band dispersions within this manifold are, however, very different from those of Na_xCoO_2. Not only is the band structure three dimensional, but also only one band approaches the top of the manifold (at X).

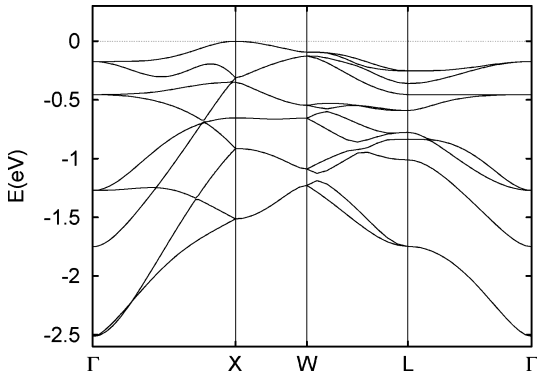

Fig. 4. Calculated valence band structure of spinel $ZnRh_2O_4$.

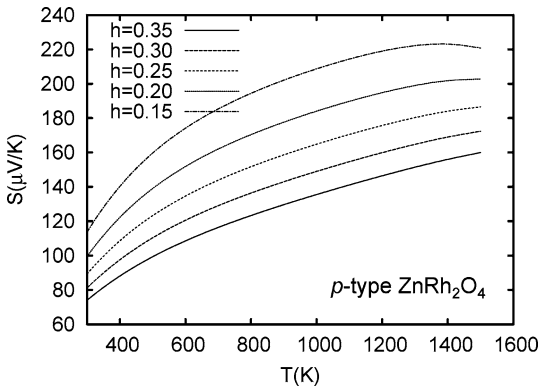

Fig. 5. Calculated $S(T)$ for cubic spinel structure $ZnRh_2O_4$ as in Fig. 3.

Nonetheless, as shown in Fig. 5, application of Boltzmann transport theory predicts that *p*-type $ZnRh_2O_4$ will have very high thermopowers, approaching those of Na_xCoO_2 at high carrier densities. Some additional results for the related rhodate $SrRh_2O_4$ and for other doping levels in $ZnRh_2O_4$ were recently reported.[18] The results show that $ZnRh_2O_4$, if doped with mobile carriers, is predicted to have a large thermopower at high metallic doping levels.

In the spinel structure the *B*-site ions are octahedrally coordinated by O, and as mentioned, there is strong hybridization between O and Rh in $ZnRh_2O_4$. The *A*-site ion (here Zn) is tetrahedrally coordinated by the same O ions. This differs from Na_xCoO_2, in which the Na ions occur in a separate layer and have (sixfold) trigonal prismatic coordination. This results in longer Na–O bond lengths than would occur in fourfold coordination. Because of these differences, it may be more difficult to dope spinels with mobile carriers than layered compounds like Na_xCoO_2. Our results show that the special properties of Na_xCoO_2 that lead to its high thermoelectric performance are the combination of narrow bands, metallic conductivity when doped, and moderate thermal conductivity. The implication is that, depending on the thermal conductivity, $ZnRh_2O_4$ and other narrow-band oxides have the potential for high thermoelectric performance if they can be effectively doped with mobile carriers.

ACKNOWLEDGEMENTS

We are grateful for helpful discussions with R. Jin, M.D. Johannes, D.G. Mandrus, I.I. Mazin, W.E. Pickett, B.C. Sales, and I. Terasaki. This work was supported by the US Department of Energy, EERE, Freedom Car and Vehicle Technologies Program.

REFERENCES

1. I. Terasaki, Y. Sasago, and K. Uchinokura, *Phys. Rev. B* 56, R12685 (1997).
2. K. Fujita, T. Mochida, and K. Nakamura, *Jpn. J. Appl. Phys.* 40, 4644 (2001).
3. H. Liligny, D. Grebille, O. Perez, A.C. Masset, M. Hervieu, C. Michel, and B. Raveau, *C.R. Acad. Sci. Paris Serie 2c* 2, 409 (1999).
4. S. Hebert, S. Lambert, D. Pelloquin, and A. Maignan, *Phys. Rev. B* 64, 172101 (2001).
5. D.J. Singh, *Phys. Rev. B* 61, 13397 (2000).
6. M.D. Johannes, D.A. Papaconstantopoulos, D.J. Singh, and M.J. Mehl, *Europhys. Lett.* 68, 433 (2004).
7. M.D. Johannes, I.I. Mazin, D.J. Singh, and D.A. Papaconstantopoulos, *Phys. Rev. Lett.* 93, 097005 (2004).
8. D. Qian, L. Wray, D. Hsieh, D. Wu, J.L. Luo, N.L. Wang, A. Kuprin, A. Fedorov, R.J. Cava, L. Viciu, and M.Z. Hasan, *Phys. Rev. Lett.* 96, 046407 (2006).
9. H.B. Yang, Z.H. Pan, A.K.P. Sekharan, T. Sato, S. Souma, T. Takahashi, R. Jin, B.C. Sales, D. Mandrus, A.V. Fedorov, Z. Wang, and H. Ding, *Phys. Rev. Lett.* 95, 146401 (2005).
10. D.J. Singh and D. Kasinathan, *Phys. Rev. Lett.* 97, 016404 (2006).
11. J.M. Ziman, *Principles of the Theory of Solids* (Cambridge: Cambridge University Press, 1972).
12. G.K.H. Madsen and D.J. Singh, *Comp. Phys. Commun.* 175, 67 (2006).
13. D.J. Singh and L. Nordstrom, *Planewaves, Pseudopotentials and the LAPW Method*, 2nd Ed. (Berlin Heidelberg New York: Springer, 2006).
14. D. Singh, *Phys. Rev. B* 43, 6388 (1991).
15. P. Blaha, K. Schwarz, G.K.H. Madsen, D. Kvasnicka, and J. Luitz, *WIE2k*, Technische Universitat Wien, 2002.
16. H. Ohta, H. Mizoguchi, M. Hirano, S. Narushima, T. Kamiya, and H. Hosono, *Appl. Phys. Lett.* 82, 823 (2003).
17. D.J. Singh, R.C. Rai, J.L. Musfeldt, S. Auluck, N. Singh, P. Kalifah, S. McClure, and D.G. Mandrus, *Chem. Mater.* 18, 2696 (2006).
18. G.B. Wilson-Short, D.J. Singh, M. Fornari, and M. Suewattana, *Phys. Rev. B* 75, 035121 (2007).